Available online at www.sciencedirect.com
ScienceDirect
Acta Materialia 55 (2007) 3081–3087
Acta MATERIALIA
www.elsevier.com/locate/actamat

Switching characteristics of MPB compositions of $(Bi_{0.5}Na_{0.5})TiO_3$–$BaTiO_3$–$(Bi_{0.5}K_{0.5})TiO_3$ lead-free ferroelectric ceramics

J. Shieh [a,*], K.C. Wu [a], C.S. Chen [b]

[a] Department of Materials Science and Engineering, National Taiwan University, 1 Roosevelt Road, Sec. 4, Taipei 106, Taiwan
[b] Department of Civil Engineering, National Taiwan University, 1 Roosevelt Road, Sec. 4, Taipei 106, Taiwan

Received 11 October 2006; accepted 4 January 2007
Available online 6 March 2007

Abstract

The polarization switching characteristics of lead-free $a(Bi_{0.5}Na_{0.5})TiO_3$–$bBaTiO_3$–$c(Bi_{0.5}K_{0.5})TiO_3$ (abbreviated as BNBK 100a/100b/100c) ferroelectric ceramics are investigated. For the first time, the strain hystereses of BNBK compositions inside and outside the morphotropic phase boundary (MPB) are presented. The total induced electrostrain ($\varepsilon_{33,total}$) and apparent piezoelectric coefficient (d_{33}) first increase dramatically and then decrease gradually as the BNBK composition moves from the tetragonal phase to the MPB and then to the rhombohedral phase. The measured polarization hystereses indicate that the BNBK compositions situated near the rhombohedral side of the MPB typically possess higher coercive field (E_c) and remanent polarization (P_r), while the compositions situated near the tetragonal side of the MPB possess higher apparent permittivity. BNBK 85.4/2.6/12 a composition well within the MPB, exhibits an $\varepsilon_{33,total}$ of ~0.14%, an apparent d_{33} of 295 pCN^{-1} and a P_r of 22.5 $\mu C\ cm^{-2}$. These property values suggest a candidate material for lead-free actuator applications.

Keywords: Ferroelectricity; Electroceramics; Perovskites; Lead-free

1. Introduction

The PZT ceramics are oxide alloys of lead, zirconium and titanium. These ceramics are high-performance ferroelectrics which possess exceptionally high and often dopant-modifiable piezoelectric coefficients ($d_{33} \approx 220$–650 pCN^{-1}) and dielectric constants ($K_{33}^T \approx 500$–5500) and have come to dominate the field of sensing, positioning, actuating and transduction applications. The high lead content of the PZT family of ceramics (~60 wt.%), however, raises grave environmental concerns. Furthermore, the high volatility of toxic lead fumes makes the PZT compounds dangerous to handle during processing. While non-lead ferroelectric ceramic systems, such as barium titanate ($BaTiO_3$) and potassium niobate ($KNbO_3$), have been known for some time, their piezoelectric and ferroelectric properties are considerably inferior.

There has been a determined effort to develop lead-free ferroelectric ceramics with high piezoelectric properties by various doping and alloying routes, but no effective alternative to the lead zirconate titanate (PZT) system has yet been found [1]. Nevertheless, several lead-free ceramic systems have shown great potential. Saito et al. [2] have developed a highly <001> textured alkaline niobate-based perovskite polycrystal with a piezoelectric charge coefficient d_{33} of 416 pCN^{-1}, which is widely regarded as the closest lead-free system to the actuator-grade hard and semi-hard PZT ceramics to date. Though, a complex processing route is required to produce Saito's highly textured polycrystal. A considerable literature also exists concerning the dielectric and piezoelectric properties of $(1-x)(Bi_{0.5}Na_{0.5})TiO_3$–$xBaTiO_3$ (abbreviated as BNBT-100x) and $(1-y)(Bi_{0.5}Na_{0.5})TiO_3$–

* Corresponding author. Tel.: +886 2 336 65287; fax: +886 2 236 34562.
E-mail address: jayshieh@ntu.edu.tw (J. Shieh).

1359-6454/$30.00
doi:10.1016/j.actamat.2007.01.012

$y(Bi_{0.5}K_{0.5})TiO_3$ (abbreviated as BNKT-100y) solid solutions [3–9]. These two bismuth sodium titanate (BNT)-based ceramic solid solutions have rhombohedral–tetragonal morphotropic phase boundary (MPB) compositions existing on $x = 0.06$–0.07 for BNBT-100x and $y = 0.16$–0.20 for BNKT-100y [8–10]. From these two BNT-based solid solutions, a ternary system, $a(Bi_{0.5}Na_{0.5})TiO_3$–$bBaTiO_3$–$c(Bi_{0.5}K_{0.5})TiO_3$ (abbreviated as BNBK 100a/100b/100c), can be developed [10]. A piezoelectric charge coefficient of $d_{33} = 191$ pCN^{-1}, an electromechanical coupling factor of $k_{33} = 0.56$ and a dielectric constant of $K_{33}^{T} = 1141$ have been observed for the BNBK 85.2/2.8/12 composition which has a tetragonal phase near the MPB [10]. In comparison with BNBT and BNKT, compositions of the BNBK ternary system typically exhibit higher depolarization and/or Curie temperatures [5,10,11]. So far the dielectric and piezoelectric properties of the BNBK system have received some limited attention [10–12]. However, there are no systematic data available on its polarization and strain hystereses.

The motivation behind the present study is to investigate the switching characteristics of environmentally friendly lead-free ferroelectric ceramics. In broad terms, ferroelectric sensors operate within the linear regime with subsequent signal amplification: linearity is more important than signal power. In other applications such as ferroelectric actuators, nonlinear behavior is a consequence of operating at high power. Hence, it is critical to measure the polarization switching characteristics of a newly developed ferroelectric system in order to gauge its ability to be used as linear and/or nonlinear devices [13]. In order to attain any commercial significance, the developed lead-free ferroelectric system must possess easy and stable processing characteristics. Based on this notion, the BNBK family of lead-free ferroelectric ceramics was chosen for the present study. Not only can the BNBK ceramics be fabricated easily via the conventional mixed-oxide route, but they also exhibit high-quality piezoelectric and dielectric properties, as documented in the existing literature [10–12]. Investigation of the switching characteristics of BNBK-based lead-free ferroelectric ceramics, focusing on the MPB compositions, is achieved through examining their hystereses in the electric polarization (D) vs. electric field (E) and strain (ε) vs. electric field (E) responses. As mentioned above, there are no systematic data available on the polarization and strain hystereses for BNBK; this insufficiency shall be addressed in the present study.

2. Experimental procedure

Conventional mixed-oxide techniques were used to prepare the BNBK ceramics. Commercially available reagent-grade metal oxide and carbonate powders were used as the starting raw materials. The types of powders used were Bi_2O_3 (Nanophase, NanoArc), Na_2CO_3 (Nacalai Tesque), $BaCO_3$ (Nacalai Tesque), K_2CO_3 (Katayama Chemical) and TiO_2 (Katayama Chemical). These oxide and carbonate powders were mixed in ethanol and ball-milled for 24 h. After calcining (800 °C, 1 h), the powder mix was again ball-milled for 24 h with the addition of PVA binder. After the second ball-milling procedure, the ground ceramic powders were oven-dried (120 °C, 24 h) and then pressed into sample discs. After debinding (600 °C, 1 h), these sample discs were sintered at 1170 °C for 2 h in air. Crystalline phases of the sintered BNBK ceramic samples were confirmed using an X-ray diffractometer (XRD; Model D/Max-B, Rigaku, Japan). The microstructures of the ceramics were analyzed via scanning electron microscopy (SEM; Model XL30, Philips, The Netherlands). In total, 11 types of BNBK composition samples were prepared and Fig. 1 shows their relative positions on the room-temperature phase diagram of the $(Bi_{0.5}Na_{0.5})TiO_3$–$BaTiO_3$–$(Bi_{0.5}K_{0.5})TiO_3$ ternary system. Samples 1–9 situate within the MPB of BNBK and consist of 40 mol% BNBT and 60 mol% BNKT. The exact constitutions of the BNBT and BNKT components of a BNBK sample are expressed by the number affixed; for example, Sample 8, which is BNBK 6.5-20, is of composition 40 mol% $(Bi_{0.5}Na_{0.5})_{0.935}Ba_{0.065}TiO_3$ + 60 mol% $Bi_{0.5}(Na_{0.8}K_{0.2})_{0.5}TiO_3$. Note that Sample 8, BNBK 6.5-20, can also be denoted as BNBK 85.4/2.6/12 by working out the exact percentages of the three constituents, $(Bi_{0.5}Na_{0.5})TiO_3$, $BaTiO_3$ and $(Bi_{0.5}K_{0.5})TiO_3$. Sample 10 (i.e., BNBK 75/5/20) and Sample 11 (i.e., BNBK 90/5/5) are two compositions outside the MPB and situate at the tetragonal and rhombohedral regions, respectively. They do not lie on the 40 mol%-BNBT–60 mol%-BNKT composition line. Several MPB compositions of the BNBT and BNKT systems were also prepared via the same processing route in this study for comparison purposes.

For polarization and strain hysteresis measurements, sample discs were cut into cuboidal specimens measuring $10 \times 10 \times 3$ mm and silver-based paints were applied onto the 10×10 mm faces to form top and bottom electrodes for electric field excitation. The top electrode was connected to ground via a ferroelectric analyzer (Model TF2000, aixACCT, Germany) for charge measurement. The bottom electrode was connected to a high voltage amplifier (Model 20/20C, Trek, USA) which supplied the electrical loading. Miniature strain gauges (Model FBX-04-11-005LE, TML, Japan) were attached onto the 10×3 mm faces of the specimen to measure strain changes in the loading direction (i.e., the 33-direction). A thin coat of epoxy resin was applied to the exposed surfaces of the strain gauges to afford extra insulation against electrical breakdown. The entire electrical loading fixture was supported in a silicon oil bath to prevent breakdown arcing. All hysteresis measurements were carried out at temperatures in the range of 20–25 °C.

3. Measurements and discussion

3.1. XRD analysis

The XRD patterns ($2\theta = 20$–$80°$) of the nine MPB compositions of BNBK prepared for this study are shown

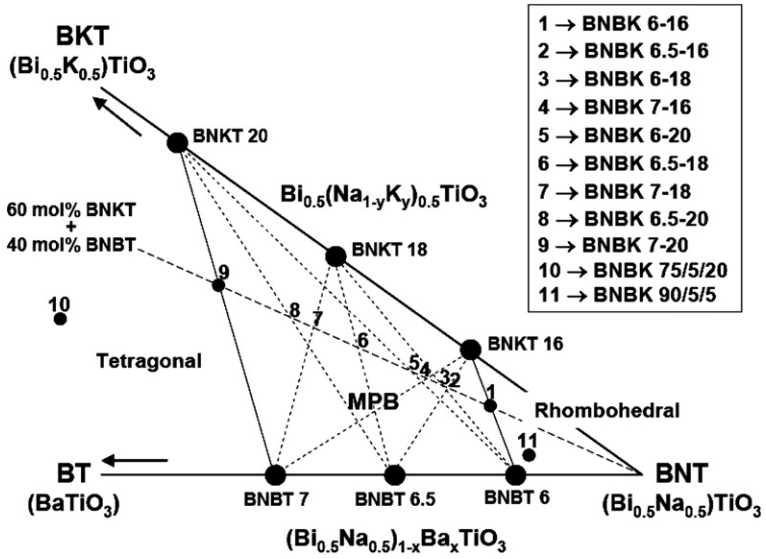

Fig. 1. Schematic of BNBK phase relationship around the MPB. Locations of 11 different BNBK composition samples prepared for the present study are shown.

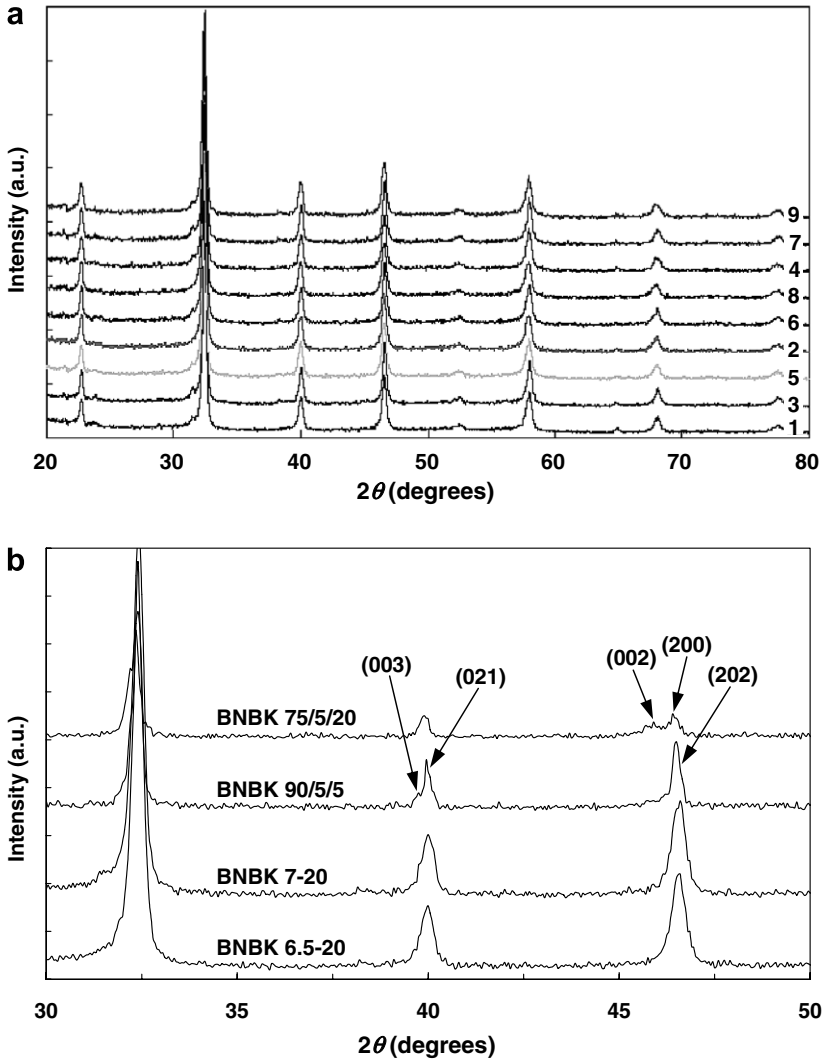

Fig. 2. (a) XRD patterns of BNBK MPB compositions at 2θ between 20° and 80° (the number attached to each pattern represents the sample number indicated in Fig. 1) and (b) XRD patterns of BNBK compositions inside and outside the MPB at 2θ between 30° and 50°.

in Fig. 2a. A single phase perovskite structure is observed for all MPB compositions, with no trace of TiO_2-nonstoichiometry-induced second phase and there are very few differences between the patterns. Fig. 2b compares the XRD patterns ($2\theta = 30$–$50°$) of four BNBK compositions – two inside the MPB (BNBK 6.5-20 and BNBK 7-20) and two outside the MPB (BNBK 75/5/20 and BNBK 90/5/5). It is evident that the crystal structure of BNBK 75/5/20 exhibits a high degree of tetragonality with the splitting of the (200) and (002) characteristic peaks at a 2θ of ~46.5°. In contrast, only the (202) peak is observed at a 2θ of ~46.5° for the heavily BNT-based BNBK 90/5/5, suggesting a rhombohedral structure. The rhombohedral symmetry of BNBK 90/5/5 is also indicated by the (003) and (021) peaks at a 2θ of ~40°. Mixtures of the (200), (002) and (202) peaks are observed in the diffraction patterns of the MPB compositions.

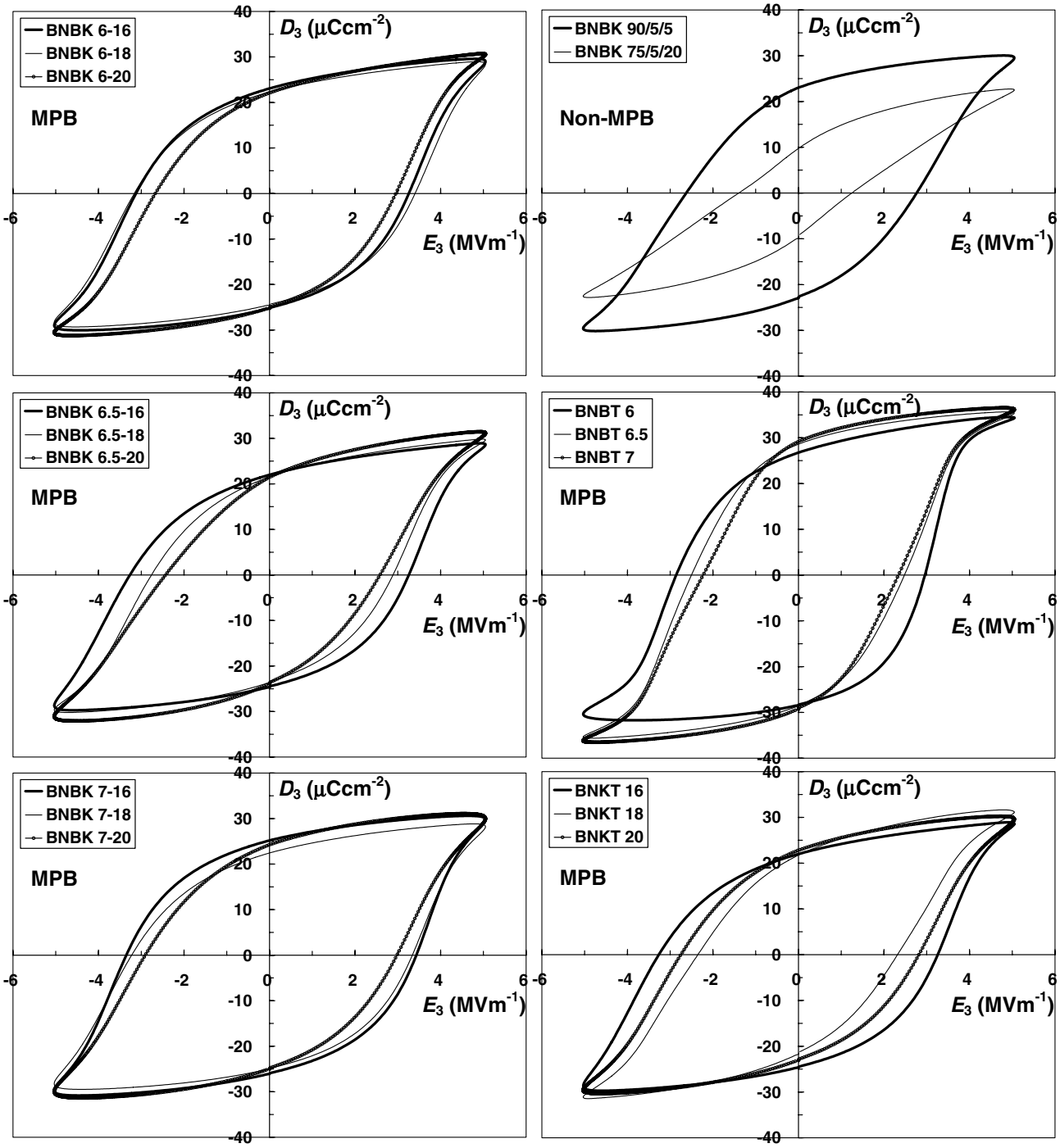

Fig. 3. Measured polarization D–E hysteresis curves for BNBK, BNBT and BNKT ($f_{app} = 0.2$ Hz).

Table 1
Coercive fields (E_c) and remanent polarizations (P_r) of BNBK, BNBT and BNKT compositions

BNBK composition	P_r (μC cm^{-2})	E_c (MV m^{-1})	Composition	P_r (μC cm^{-2})	E_c (MV m^{-1})
6-16	24.0	3.2	BNBK 90/5/5	22.8	2.7
6-18	23.3	3.3	BNBK 75/5/20	9.5	1.3
6-20	23.4	2.8			
6.5-16	23.3	3.3	BNBT 6	27.4	2.9
6.5-18	22.5	2.8	BNBT 6.5	28.5	2.5
6.5-20	22.5	2.5	BNBT 7	29.1	2.3
7-16	25.5	3.4	BNKT 16	23.3	3.3
7-18	23.6	3.3	BNKT 18	21.6	2.3
7-20	24.5	3.0	BNKT 20	22.8	2.8

3.2. Polarization hysteresis

The stable polarization *D-E* hysteresis curves for the BNBK, BNBT and BNKT specimens, measured at a cyclic electric field of amplitude ±5.0 MV m^{-1}, a frequency of 0.2 Hz and sinusoidal waveform, are shown in Fig. 3. The coercive fields (E_c) and remanent polarizations (P_r) of the specimens obtained from the measured *D–E* curves are listed in Table 1. It is evident from Fig. 3 and Table 1 that the BNBK specimens of MPB compositions (e.g., BNBK 7-20) typically display more noticeable ferroelectric characteristics than those of compositions outside the MPB (e.g., BNBK 75/5/20) with higher P_r values and sharper polarization switchings.

If only the MPB compositions are considered, the measurements shown in Fig. 3 indicate that BNBT is the "softest" among the three ferroelectric systems, with its specimens showing the highest average P_r and lowest average E_c. Saturation of polarization at high electric fields, indicated by the long "tails" of the *D–E* hysteresis curves, is apparent in the BNBT specimens. In contrast, the BNKT specimens exhibit the lowest average P_r and a less sharp polarization transition at E_c (i.e., switching is completed over a wider range of electric field) – both are indications of a "hard" ferroelectric system. The switching behavior of BNBK in terms of hardness/softness falls in between the BNBT and BNKT systems and is strongly dependent on its composition. In all three systems, the specimens with compositions situated at or near the rhombohedral side of the MPB (e.g., BNBT-6, BNKT-16, BNBK 6-16, BNBK 6.5-16, BNBK 6-18 and BNBK 7-16) exhibit larger polarization hystereses, which typically give rise to higher E_c and P_r values, while the compositions situated at or near the tetragonal side of the MPB (e.g., BNBT-7, BNKT-20, BNBK 7-20 and BNBK 6.5-20) possess higher apparent permittivity, which could be calculated from the slope gradient of the *D-E* hysteresis curve at zero electric field. Among the nine MPB compositions of BNBK prepared for this study, BNBK 6.5-20 had the lowest E_c (=2.5 MV m^{-1}), BNBK 7-20 had a relatively high P_r (=24.5 μC cm^{-2}) with an E_c just below 3.0 MV m^{-1} and BNBK 7-16 exhibited the largest P_r (=25.5 μC cm^{-2}) and E_c (=3.4 MV m^{-1}) values.

3.3. Strain hysteresis

The stable strain *ε–E* hysteresis curves (i.e., butterfly curves) for the BNBK compositions inside and outside the MPB, measured at a cyclic electric field of amplitude ±5.0–5.5 MV m^{-1}, a frequency of 0.2 Hz and sinusoidal

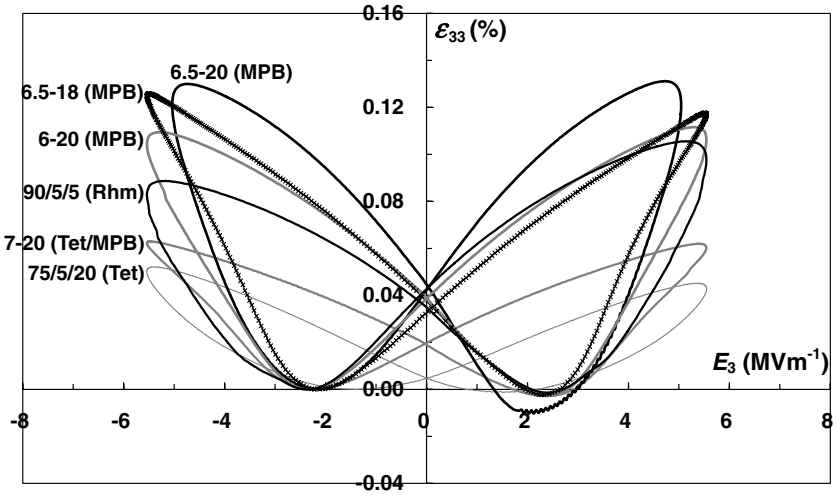

Fig. 4. Measured strain *ε–E* hysteresis curves for BNBK compositions inside and outside the MPB (f_{app} = 0.2 Hz).

waveform, are shown in Fig. 4. In order to achieve a satisfactory level of polarization saturation with 5.0–5.5 MV m^{-1}, only the BNBK compositions with $E_c < 3.0$ MV m^{-1} were chosen for the strain hysteresis analysis. Note that ±15 kV is needed to achieve ±5.0 MV m^{-1} on the 3 mm thick specimen. Strain measurements with excitation voltage >15 kV were not carried out in order to protect the strain amplifier and gauges from high-voltage arc striking. It is evident from Fig. 4 that the tetragonal BNBK produces relatively the smallest strain under cyclic electrical loading. The remanent strain (ε_r) and total electrostrain in the 33-direction ($\varepsilon_{33,total}$) increase significantly when the BNBK composition moves from the tetragonal phase into the MPB, peaking at BNBK 6.5-20. While ε_r remains relatively unchanged, $\varepsilon_{33,total}$ decreases progressively as the composition shifts away from the MPB BNBK 6.5-20 into the rhombohedral phase, which is achieved by increasing the amount of BNT in the BNBK system. Fig. 4 shows that MPB compositions BNBK 6.5-18 and BNBK 6-20, which contain more BNT than BNBK 6.5-20, exhibit smaller electrostrains. A similar trend to $\varepsilon_{33,total}$ is also observed for the apparent d_{33}, obtained from the slope gradient of the butterfly curve at zero electric field. With a composition well within the MPB, BNBK 6.5-20 exhibits an $\varepsilon_{33,total}$ of ~0.14%, more than double than that of BNBK 7-20 which situates at the tetragonal boundary of the MPB. The apparent d_{33} of BNBK 6.5-20 is 295 pCN^{-1}, an impressive number for a lead-free ferroelectric ceramic. The values of $\varepsilon_{33,total}$ and apparent d_{33} for the compositions chosen for the strain hysteresis analysis are listed in Table 2.

The stable polarization and strain hysteresis curves for BNBK 90/5/5 and BNBK 75/5/20 are shown in Figs. 3 and 4, respectively. Apart from the actuating properties such as $\varepsilon_{33,total}$ and d_{33}, the heavily BNT-based rhombohedral BNBK 90/5/5 also displays a much higher remanent polarization than the tetragonal BNBK 75/5/20. This is most likely due to the higher number of equivalent crystallographic directions which the spontaneous polarization could take up in a rhombohedral structure (i.e., eight [111] directions). Nevertheless, the magnitude of strain produced by BNBK 90/5/5 is still no match for those produced by the compositions well within the MPB.

Table 2
Total electrostrains ($\varepsilon_{33,total}$) and apparent piezoelectric coefficients (d_{33}) of selected BNBK, BNBT and BNKT compositions

BNBK composition	Crystallographic phase	$\varepsilon_{33,total}$ (%)	Apparent d_{33} (pCN^{-1})
75/5/20	Tetragonal	0.052	76
7-20	Tetragonal/MPB	0.064	121
6.5-20	MPB	0.140	295
6.5-18	MPB	0.126	216
6-20	MPB	0.114	209
90/5/5	Rhombohedral	0.107	205
Other composition			
BNBT 6.5	MPB	0.198	361
BNKT 20	Tetragonal/MPB	0.054	97

Fig. 5 compares the strain hystereses of BNBK 6.5-20 and its two constituent components, BNBT-6.5 and BNKT-20. A substantial 0.20% total electrostrain is observed for BNBT-6.5, a composition positioned right in the middle of the MPB of the BNBT system. When BNKT-20 is introduced into BNBT-6.5 (i.e., forming BNBK 6.5-20), decreases in the electrostrain and apparent d_{33} are obvious. This decline of actuating ability, though, is likely to be rewarded by increases in the depolarization and Curie temperatures (20–80 °C increase, depending on composition), as indicated by existing studies [5,10,11]. The pure BNKT composition, BNKT-20, exhibits a small $\varepsilon_{33,total}$ of ~0.05%, much less than those of BNBT-6.5 and BNBK 6.5-20. The values of $\varepsilon_{33,total}$ and apparent d_{33} for BNBT-6.5 and BNKT-20 are also listed in Table 2. It is clear from Fig. 5 that the strain hysteresis of a BNBK composition combines the straining characteristics of its two constituent components, BNBT and BNKT. The

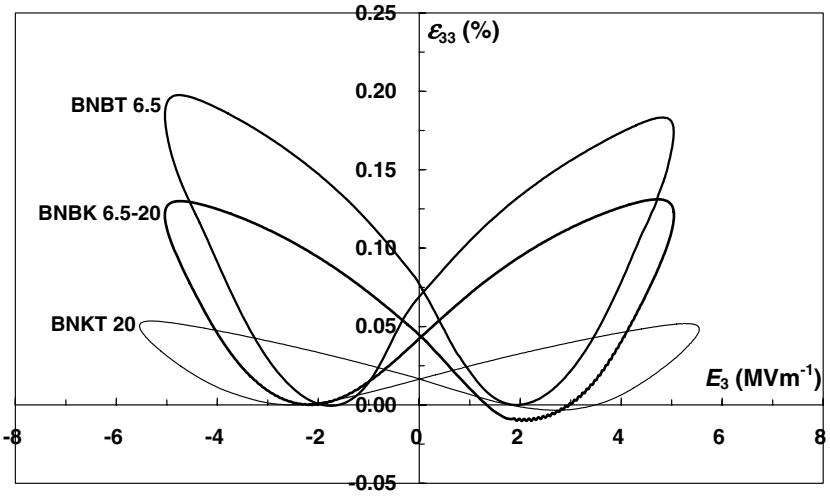

Fig. 5. Measured strain ε–E hysteresis curves for BNBT-6.5, BNKT-20 and BNBK 6.5-20 ($f_{app} = 0.2$ Hz).

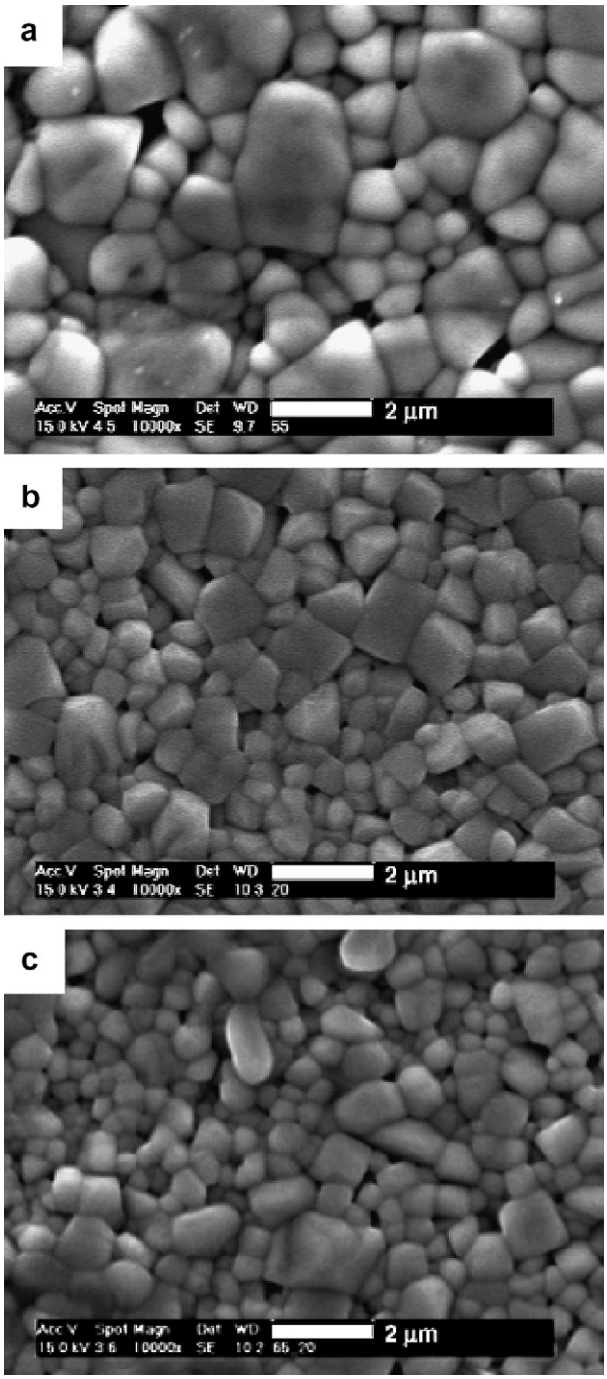

Fig. 6. SEM micrographs of (a) BNBT-6.5, (b) BNKT-20 and (c) BNBK 6.5-20 ceramics.

SEM images of the microstructures of the BNBT-6.5, BNKT-20 and BNBK 6.5-20 ceramics are shown in Fig. 6. No significant differences are observed between the microstructures except that BNBT-6.5 has a slightly larger grain size and BNKT-20 has a more rectangular grain shape. The grain size of the three ceramics is ~0.5–2.5 μm. It is evident from Fig. 6 that when BNKT-20 is introduced into BNBT-6.5 (i.e., forming BNBK 6.5-20), grain growth is suppressed and the grain shape becomes more rectangular.

4. Conclusion

In summary, the switching characteristics of the MPB compositions of the $(Bi_{0.5}Na_{0.5})TiO_3$–$BaTiO_3$–$(Bi_{0.5}K_{0.5})$-TiO_3 lead-free system have been investigated. This was achieved through examining their polarization and strain hystereses. The BNBK compositions situated near the rhombohedral side of the MPB typically possess higher E_c and P_r, while the compositions situated near the tetragonal side of the MPB possess higher apparent permittivity. The total induced electrostrain and apparent d_{33} increase dramatically when the BNBK composition moves from the tetragonal phase into the MPB. They then decrease gradually as the composition shifts away from the MPB into the rhombohedral phase. When BNKT is introduced into BNBT (i.e., forming BNBK), decreases in the electrostrain and apparent d_{33} are evident. The strain hysteresis of a BNBK composition combines the straining characteristics of its two constituent components, BNBT and BNKT. Under an alternating electric field of ± 5.0 MV m^{-1}, BNBK 6.5-20 (a.k.a. BNBK 85.4/2.6/12) exhibits an $\varepsilon_{33,total}$ of ~0.14%, an apparent d_{33} of 295 pCN^{-1}, an E_c of 2.5 MV m^{-1} and a P_r of 22.5 μC cm^{-2}. These notable ferroelectric property values indicate that the BNBK 6.5-20 ceramic is a candidate material for lead-free actuator applications.

Acknowledgement

The authors are grateful for the financial support of the National Science Council (NSC) of Taiwan under contract numbers NSC94-2218-E-002-062 and NSC94-2216-E-002-019.

References

[1] Takenaka T, Nagata H. J Eur Ceram Soc 2005;25:2693.
[2] Saito Y, Takao H, Tani T, Nonoyama T, Takatori K, Homma T, et al. Nature 2004;432:84.
[3] Kundu A, Soukhojak AN. Appl Phys A 2006;82:309.
[4] Qu Y, Shan D, Song J. Mater Sci Eng B 2005;121:148.
[5] Wang XX, Or SW, Tang XG, Chan HLW, Choy PK, Liu PCK. Solid State Commun 2005;134:659.
[6] Wang XX, Kwok KW, Tang XG, Chan HLW, Choy CL. Solid State Commun 2004;129:319.
[7] Ishii H, Nagata H, Takenaka T. Jpn J Appl Phys 2001;40:5660.
[8] Sasaki A, Chiba T, Mamiya Y, Otsuki E. Jpn J Appl Phys 1999;38:5564.
[9] Takenaka T, Maruyama K, Sakata K. Jpn J Appl Phys 1991;30:2236.
[10] Nagata H, Yoshida M, Makiuchi Y, Takenaka T. Jpn J Appl Phys 2003;42:7401.
[11] Wang XX, Choy SH, Tang XG, Chan HLW. J Appl Phys 2005;97:104101.
[12] Wang XX, Tang XG, Chan HLW. Appl Phys Lett 2004;85:91.
[13] Shieh J, Huber JE, Fleck NA. Acta Mater 2003;51:6123.